Monte Carlo Simulation of Diffusion and Reaction in Two-Dimensional Cell Structures

Mark R. Riley,* Helen M. Buettner,* Fernando J. Muzzio,* and Sebastian C. Reyes‡
*Department of Chemical and Biochemical Engineering, Rutgers University, Piscataway, New Jersey 08855, and ‡Corporate Research Laboratories, Exxon Research and Engineering Company, Annandale, New Jersey 08801 USA

ABSTRACT Diffusion and reaction processes control the dynamics of many different biological systems. For example, tissue respiration can be limited by the delivery of oxygen to the cells and to the mitochondria. In this case, oxygen is small and travels quickly compared with the mitochondria, which can be considered as immobile reactive traps in the cell cytoplasm. A Monte Carlo theoretical investigation quantifying the interplay of diffusion, reaction, and structure on the reaction rate constant is reported here for diffusible particles in two-dimensional, reactive traps. The placement of traps in overlapping, nonoverlapping, and clustered spatial arrangements can have a large effect on the rate constant when the process is diffusion limited. However, under reaction-limited conditions the structure has little effect on the rate constant. For the same trap fractions and reactivities, nonoverlapping traps have the highest rate constants, overlapping traps yield intermediate rate constants, and clustered traps have the lowest rate constants. An increase in the particle diffusivity in the traps can increase the rate constant by reducing the time required by the particles to reach reactive sites. Various diffusive, reactive, and structural conditions are evaluated here, exemplifying the versatility of the Monte Carlo technique.

NOTATION

CT	= Clustered traps
D_c	= Diffusivity in traps
D_e	= Effective diffusivity
D_e/D_0	= Normalized effective diffusivity
D_p	= Particle diffusivity
D_t	= Trap diffusivity
D_0	= Diffusivity in continuous phase
D_0/D_c	= $1/\gamma$ - Diffusivity ratio
D^*	= Scaled diffusivity
k	= Calculated rate constant
k_r	= Intrinsic trap rate constant
k_s	= Smoluchowski rate constant
L	= Edge length of the placement domain
NT	= Nonoverlapping traps
OT	= Overlapping traps
P	= Reaction probability
r_p	= Particle radius
r_t	= Trap radius
S_a	= Trap surface area
ϵ	= Random variable [0,1]
λ_c	= Mean step size in the trap phase
λ_0	= Mean step size in the continuous phase
ϕ	= Area fraction of traps
Φ	= Volume fraction of traps

INTRODUCTION

Coupled diffusive and reactive mechanisms control the behavior of many biological processes. Diffusion results from random molecular motion and frequently plays a major role in chemical reactions by controlling the rate at which reactive species are brought into contact at molecular scales. Chemical reactions often depend strongly on the concentration of reactants in the neighborhood of reactive sites. The relative rates of these mechanisms determine whether the overall process is diffusion or reaction limited. Diffusive restrictions have been identified as the limiting factor in numerous biological processes such as the delivery of nutrients to tumor cells (Freyer and Sutherland, 1986), the rate of oxygen uptake by red blood cells (Coin and Olson, 1979), coagulation of clotting factors (McGee et al., 1992), calcium signaling in smooth muscle cells (Kargacin, 1994), and reactions between G-proteins and receptors (Mahama and Linderman, 1994). The consumption rate of oxygen and nutrients by several cell types has been reported to be in the range of $1.4–6.0 \times 10^{-17}$ mol/cell-s (Fleishaker and Sinskey, 1981; Sutherland and Durand, 1984; Wohlpart et al., 1990; Ozturk and Palsson, 1991; Glacken et al., 1988). Structural effects, such as the distribution of reactive sites, can also strongly influence the behavior of these systems. For example, 1) in cultured hepatocytes, many of the mitochondria can be found arranged in small clusters, and this clustering can be an important factor in determining the intracellular supply of oxygen to the mitochondria (Jones, 1984); 2) cell surface receptors aggregate on cell membranes, effectively reducing the surface area available to interact with ligands (Baldo et al., 1991; DeFelice, 1993); and 3) the oxygen distribution in aerobic biofilms is strongly correlated to clustering of microbial cells (de Beer et al., 1994).

These studies have raised intriguing questions about the mechanisms and rates of diffusive and reactive processes in biological systems. Does the material structure (i.e., placement of reactive traps) have an effect on the diffusion and reaction processes, and if so, under what conditions will

Received for publication 19 September 1994 and in final form 1 February 1995.

Address reprint requests to Dr. Helen M. Buettner, Department of Chemical and Biochemical Engineering, Rutgers University, PO Box 909, Piscataway, NJ 08855–0909. Tel.: 908-445-2231; Fax: 908-445-5313; E-mail: buettner@zodiac.rutgers.edu.

0006-3495/95/05/1716/11 $2.00

structural effects be largest (or smallest)? What type of structure has the highest reactivity? Could two systems with different microscopic reactive and structural conditions have similar macroscopic rates of reaction? How would changes in molecular diffusivity affect the overall reactivity? In this paper we examine a variety of diffusive, reactive, and structural conditions for their effect on the reactive behavior of a general biological system involving numerous highly mobile species (e.g., nutrients, ligands) diffusing in a material with large immobile traps (e.g., cells, receptors) distributed in an inert continuous phase. This can be interpreted either as a single cell with distributed reactive sites or as multiple metabolizing cells immobilized within a matrix, such as in tissue. Microstructural details are represented as different trap arrangements; the traps may be uncorrelated (random) or highly correlated (clustered), and they may penetrate each other (overlapping) or be impenetrable (nonoverlapping). Monte Carlo (MC) computational methods are used here to investigate trends and conditions not easily measured experimentally.

MC simulations have been successfully used by several investigators to study diffusion in biological systems. Saxton (1989, 1992, 1993a,b, 1994) developed MC techniques to investigate lateral particle diffusion in the presence of various immobile obstacles on a two-dimensional triangular lattice representing the cell membrane. Dwyer and Bloomfield (1993) studied particle diffusion in concentrated solutions of DNA and protein while accounting for interactions on the molecular level. El-Kareh and co-workers (1993) calculated effective diffusivities of monoclonal antibodies in simulated tissue. These diffusivities were insensitive to alterations in the placement and distance between cells.

The addition of reactions introduces another level of complexity to the analysis of transport in biological systems, particularly when the process is diffusion limited. A process is reaction limited when the reaction requires significantly more time than that needed for diffusive transport. Such systems are usually homogeneous. A process is diffusion limited when the rate-limiting step is bringing together mutually reactive species, the reaction requiring negligible time by comparison. Diffusion-limited systems often display steep concentration gradients. In this case, the process is inhomogeneous and both the structural characteristics and reaction kinetics of the system must be taken into account. When reactions are fast and the trap density is low, the diffusion-controlled rate constant, k_s, can be estimated by the Smoluchowski limit (Berg and von Hippel, 1985). This expression describes the transport of uniformly distributed particles to a single perfectly absorbing trap (Berg and von Hippel, 1985) and takes the form:

$$k_s = 4\pi(D_p + D_t)(r_p + r_t), \tag{1}$$

where D_p is the diffusivity of the particles, D_t is the diffusivity of the trap, r_p is the particle radius, and r_t is the trap radius. The reaction rate constant is maximized when one species is very large and the other species moves rapidly. For small particles ($r_p \ll r_t$) diffusing in a system of large, immobile traps ($D_p \gg D_t$), the Smoluchowski limit can be expressed as:

$$k_s = 4\pi D_p r_t. \tag{2}$$

This approximation assumes that there are no interactions between traps; i.e., the supply of reactive particles to a trap is unaffected by the presence of other traps. This condition is usually achieved for small fractions of traps. The Smoluchowski limit becomes increasingly inaccurate as reactions become slower and as the trap fraction becomes large so that interactions and spatial arrangements of traps become important. As biological systems often display high fractions of reactive traps distributed in a complex manner (Karel et al., 1985; de Beer et al., 1994), Eq. 2 is not particularly accurate but can be used to make a first approximation to the rate constant.

Theoretical investigations have evaluated diffusion and reaction while accounting for interactions of traps at high fractions to provide estimates of the rate constant of diffusing particles reacting with stationary traps. The rate constant (k) has been correlated to the trap volume fraction and distribution functions for the trap locations for specific types of structure (Muthukumar, 1982; Cukier and Freed, 1983; Fixman, 1984; Rubinstein and Torquato, 1988). Presently, however, no general purpose analytical formula is available for predicting the diffusive and reactive properties for variable phase properties and volume fractions (Kim and Torquato, 1991).

MC simulations have been developed to calculate rate constants for reactive particles diffusing in some complex structures (Richards, 1986a,b, 1987; Zheng and Chiew, 1989, 1990; Lee et al., 1989; Miller and Torquato, 1989; Miller et al., 1991; Zhao and Reichert, 1994). In these previous studies, particles undergo a simulated random walk and react instantaneously upon reaching the surface of a trap. The probability of reaction, P, is 1 and particles never enter the traps. Results from these studies apply to some biological systems such as several types of fluorescence quenching (Joshi et al., 1990; Szabo, 1989), but there are numerous other systems for which reactions occur more slowly. For example, Northrup and Erickson (1992) reported that antibody-antigen complexation occurs with a rate constant three orders of magnitude lower than the Smoluchowski rate. For diffusion in cells, the probability that a molecule (particle) will react inside the cell (or trap) is generally less than 1 because reactions are not instantaneous (see Fig. 1). When oxygen reaches a cell surface, it generally does not react instantaneously; it penetrates the cell and reacts inside the mitochondria after some diffusion time. Such situations, although relevant to many biological applications, have been much less studied. Exceptions include the work of Fixman (1984) and Torquato and Avellaneda (1991), who investigated high reaction probabilities of 0.6666 and 0.1, respectively. Additionally, Axelrod and Wang (1994) studied cell surface receptors that bind ligands with a small success probability of 0.001, assuming that only a small fraction of ligand-receptor collisions lead to binding. These studies did not

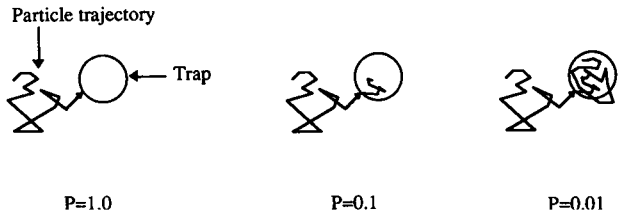

FIGURE 1 Schematic random walk trajectory displaying the effect of trap reactivity (P) on particle reaction in a trap. When $P = 1$, particles react on the trap surface. For $P < 1$, particles may diffuse into and through the trap to an extent that depends on P. Particle step lengths are much shorter than those displayed here.

evaluate the effect of structure on the reactive properties. Molecules would bounce off of a trap if they did not react with the trap. Another aspect not addressed is that reactive molecules can diffuse into cells and often have a lower diffusivity in the cells (D_c) than they have in the environment outside the cells (D_0). Diffusivity ratios (D_0/D_c) typically are in the range between 2 and 5 (Westrin and Axelsson, 1991). The differences between values of D_0 and D_c are primarily a result of the increased obstructional effects found inside the cell and possibly because of additional nonspecific binding inside a cell, both of which would hinder the progress of a diffusing species.

In a previous study, we focused exclusively on the diffusion of small molecules in immobilized cell systems, in which both the cells and the extracellular support matrix allowed some measure of transport (Riley et al., 1995). For conditions relevant to cells immobilized in a single, continuous support phase, the structure (such as the arrangement of cells in nonoverlapping, overlapping, or clustered schemes) was found to have negligible effect on the diffusivity of small molecules. Additionally, for a wide range of volume fractions (Φ) and diffusivity ratios (D_0/D_c), the normalized diffusivity of a molecule could be accurately described by the relationship:

$$D^*(\Phi) = (1 - D_e(\Phi)/D_0)/(1 - D_c/D_0), \quad (3)$$

where $D^*(\Phi)$ is a scaled diffusivity and $D_e(\Phi)$ is the effective diffusivity. $D(\phi)$ is well represented by a simple empirical relation:

$$D^*(\Phi) = 1.7271\Phi - 0.8177\Phi^2 + 0.09075\Phi^3 \quad (4)$$

This scaling removes the dependence of the effective diffusivity on the diffusivity ratio and permits the evaluation of the effective diffusivity solely in terms of the volume fraction of cells. These relations provide an accurate means to extrapolate diffusivity measurements from one set of conditions to another, i.e., for changing cell fraction, cell type, or diffusing solute (Riley et al., 1994). The predictions of Eq. 4 are in good agreement with experimental diffusivities in the literature.

Although the material structure is unimportant for purely diffusive conditions, the results presented in this paper show that the structure can significantly affect the behavior of a reactive system. A MC approach (described in the next section, Algorithms) is used to investigate the effect of reaction probability (P), particle diffusivity, and material structure on diffusion and reaction of particles in a two-dimensional material consisting of traps of identical size. Both perfect ($P = 1.0$) and imperfect ($P < 1.0$) absorbers are considered. Two-dimensional systems are investigated primarily because of ease of computation. A two-dimensional system permits a more comprehensive description of the material structure than can be obtained in a three-dimensional system for the same computer memory capacity. In addition, it offers insight into carrying out computations in three dimensions. In future communications, we shall describe such three-dimensional calculations. The results presented in Results and Discussion show that structure plays an important role in the overall reactive behavior for diffusion-limited conditions but only moderately so for reaction-limited conditions.

ALGORITHMS

The MC algorithm described here is similar to those previously used to investigate diffusion and reaction in multiphase systems (Richards, 1987; Zheng and Chiew 1989; Lee et al., 1989). The continuum method used here adapts our previous study of diffusion (Riley et al., 1994, 1995) to account for diffusion of particles through both phases and reaction throughout the traps.

Structural representation

Material structures are simulated by using simple rules to determine the placement of the traps. Circular traps of uniform size are placed in a square domain with periodic boundaries so that if a trap intersects a boundary it partially reappears across the opposite boundary. This procedure effectively simulates an infinitely large structure. Trap coordinates are produced by using a random number generator and a specific set of placement rules so that the entire structure is specified by the center coordinates and the diameter of the traps. Traps are positioned one at a time until a desired area fraction is achieved. The method can be used to simulate various structural features depending on characteristics such as the trap geometry, trap size, whether the traps are isolated or clustered, and whether the traps overlap or do not overlap. We investigate three basic types of structure (Fig. 2) that can be classified as nonoverlapping traps (NT), overlapping traps (OT), and clustered traps (CT).

Nonoverlapping traps

NT structures are generated by positioning NTs one at a time into a square domain of side length L until the desired area coverage is attained. Traps are checked for overlap with previously placed traps; overlapping positions are rejected and new coordinates are obtained for the misplaced trap. The fraction of traps follows:

$$\phi = N\pi r_t^2/L^2, \quad (5)$$

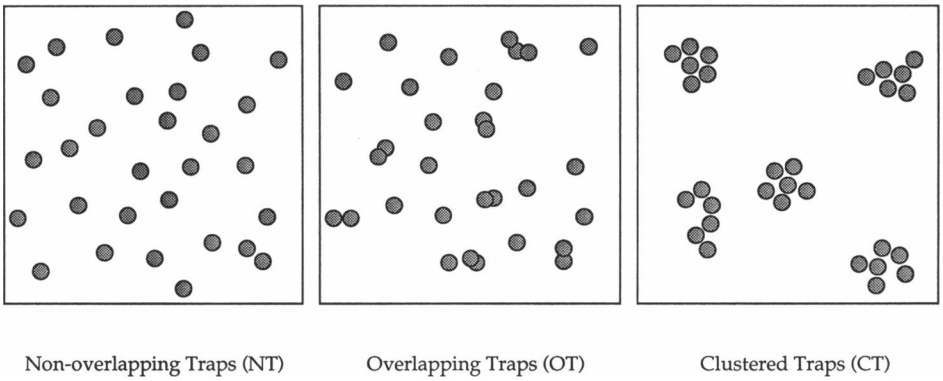

FIGURE 2 Schematic representation of the three types of trap placement investigated here.

where ϕ is the area fraction of traps, N is the number of traps, r_t is the radius of an individual trap, and L is the length of the domain. The maximum fraction without overlap investigated here is 0.50. The experimental parking limit is approximately 0.55 for circles in two dimensions (Onoda and Liniger, 1986).

Overlapping traps

An OT system is obtained by randomly positioning traps in the placement region without regard to whether new traps overlap with previously existing traps. This method of placement can reach trap fractions up to unity. The trap fraction is counted as the true area fraction of trap coverage; overlapping regions are counted only once regardless of how many traps are positioned over the area. The trap fraction follows the Poisson relation (Chiew and Glandt, 1983):

$$\phi = 1 - \exp[-N\pi r_t^2/L^2]. \quad (6)$$

Clustered traps

A CT structure is generated by a simple cluster growth process that sequentially adds NTs adjacent to previously placed traps (Riley et al., 1995). First, an initial seed trap is placed randomly in the support. A second trap is then placed at a random angular position adjacent to the first trap with center coordinates separated by 1.01 times the trap diameter. This separation ensures that cells are very close together, as observed in the growth of immobilized cells, but the simulation will still recognize the cells as distinct and nonoverlapping. A third trap is then placed at a random angle, next to the first trap. The new trap is not allowed to overlap with any existing traps; overlapping positions are rejected, and the overlapping trap is replaced. New traps are placed in a similar fashion next to existing traps until the appropriate number of traps for the cluster have been positioned. Trap fractions are controlled by changing the number of clusters while keeping the trap diameter and the cluster size constant. Clusters of 50 traps produced by this method are roughly circular in shape. Jones (1984) has reported that in a liver cell line mitochondria can be observed in clusters containing up to 50 mitochondria.

In these structures, the trap diameter is uniform at 15 nodes per trap. These traps represent some mammalian cell types, such as hybridomas, which have a diameter of approximately 10 μm. One computational node corresponds to approximately 0.6667 μm. The placement domain is essentially infinite in size because of periodicity in the boundaries. The length of each border on the unit square is 1000 nodes or 66 times the diameter of a trap. The average distance between the center of a trap and the center of its nearest neighbor for nonoverlapping and overlapping structures is reported in Table 1. These distances have been divided by the diameter of a trap to normalize results. Note that for overlapping traps with $\phi \geq 0.70$, this average distance between traps is less than 1 because of the interpenetration of traps. We report the average distance between a cluster and its nearest neighboring cluster (Table 1). These distances have been normalized by the trap diameter. For high trap fractions ($\phi \geq 0.40$) clusters are tightly packed together with a separation distance of approximately one trap.

The model of cell placement is based on previous models of the proliferation of anchorage-dependent cells on a surface (Zygourakis et al., 1991a,b) and of cells immobilized on microcarriers (Hawboldt et al., 1994). At high cell densities ($\phi > 0.60$) the structures resemble closely packed cells in a tissue such as tumor nodules that can have cell fractions of approximately 50–90 volume percent (Carlsson and Yuhas, 1984; Carlsson and Brunk, 1977).

TABLE 1 Average shortest distance between traps in NT structures, between traps in OT structures, and between clusters in CT structures

NT fraction	Distance	OT fraction	Distance	CT fraction	Cluster distance
0.10	3.19	0.10	2.89	0.10	4.20
0.20	2.35	0.25	1.73	0.20	2.05
0.30	1.97	0.40	1.29	0.30	1.17
0.40	1.76	0.55	1.02	0.40	1.06
0.50	1.61	0.70	0.83	0.50	1.01
		0.90	0.60		

Distances are reported in terms of trap diameters, here 15 nodes per trap.

Random walk simulation

The overall rate constant for reaction between particles and traps is determined by the average time required for particles to travel from their initial position to the position where they react (see Fig. 1). Tracers are initiated at random positions in the structure, both inside and outside traps. Diffusion outside the traps is modeled as a series of steps in random directions with step length $\lambda = -\lambda_0 \log\epsilon$, where ϵ is a random number with uniform probability in the interval (0,1) and λ_0 is the average step size. This logarithmic step size distribution follows from the survival equation from the kinetic theory of gases (Tabor, 1969) and is commonly used in many diffusive MC studies (Reyes and Iglesia, 1991). The logarithmic step distribution produces diffusivities in agreement with several rigorous theoretical models of diffusion in heterogeneous materials (Riley et al., 1995). Although the logarithmic step distribution applies specifically to diffusion of gases, rate constants calculated with the logarithmic step distribution are identical to those calculated by using a constant step size, which has been previously used for studies of diffusion in condensed systems (Saxton, 1989). The mean step length, λ_0, is less than 0.035 times the cell diameter to minimize finite cell size effects. Particles inside the traps take steps with sizes $\lambda = -\gamma\lambda_0 \log\epsilon$, where $\gamma = D_c/D_0$ is a constant less than 1, representing the decrease in diffusivity inside the traps relative to the diffusivity in the surrounding material. Oxygen has a diffusivity of approximately 3×10^{-5} cm^2/s in water (Vaupel, 1976) and approximately $0.75–1.75 \times 10^{-5}$ cm^2/s inside some types of cells (Vaupel, 1976; Grote et al., 1977). Additional experimental evidence in the literature suggests that the diffusivity of oxygen in some cell types is approximately 25% of that in water or in a solidified gel (Ho and Ju, 1988; Libicki et al., 1988). Also, DeBacker et al., (1992) and Scott et al. (1989) reported D_0/D_c for glucose in immobilized cells to be approximately 3. We have used a diffusivity ratio of $D_0/D_c = 4$, except where indicated otherwise.

As the length of individual steps along the random walk depends on whether the particle is inside a trap or in the surrounding material, at each step one must know the particle position relative to the traps. To accomplish this, the placement domain is discretized into an array of 1000 × 1000 nodal points. The discretization procedure is similar to that previously used by Lee and Torquato (1988) to determine the porosity of two-phase disordered media. Note that traps are not placed at regular lattice positions. The structural representation consists of three types of sites (Fig. 3): continuous phase sites (with $D = D_0$ and $P = 0$), nonreactive trap sites (with $D = D_c$ and $P = 0$), and reactive trap sites (where particles are consumed with $P = 1.0$). To avoid finite size effects, traps are small compared with the area of the placement domain, but each trap encloses a relatively large number of nodes, so that the perimeter of the trap can be adequately described. A diameter of 15 nodes per trap is used, except where indicated otherwise. The reactive sites are randomly distributed throughout an individual trap and correspond to one square node each. The reaction probability is the fraction of trap nodes that are reactive. When $P = 1.0$, traps are perfect absorbers and 100% of the trap is covered with reactive sites so that particles react immediately upon contacting the surface of a trap. When $P = 0.1$, then 10% of the nodes inside the trap are reactive sites (see Fig. 3). When $P < 1.0$, a particle in contact with a trap may not immediately react; it may diffuse into the trap and react in its interior or it may diffuse out of the trap. Nonreactive nodes within a trap are computationally assigned a diffusivity of D_c. Nodes outside of the traps are assigned a diffusivity of D_0. To determine whether a node inside a trap is to be reactive, a random number (0,1) is selected. If this number is less than the assigned reaction probability, P, then the node is deemed reactive. This scheme leads to fluctuations in the number of reactive nodes per trap. The diffusing particles perform a random walk through the material and the immediate environment of a particle is determined by recalling the type of the node nearest to the particle. If the node is reactive, the particle reacts, and another particle is initiated. Particles are allowed to randomly begin on reactive sites, in which case their time to react is zero. The time (t) for a particle to diffuse from its initial position to the site where it reacts is used to compute the rate constant, $k = 1/t$, averaged for 1000 particles, each walking through at least 50 structural realizations for each condition. This ensures that the standard deviation is less than 5% of the mean, typical for MC simulations.

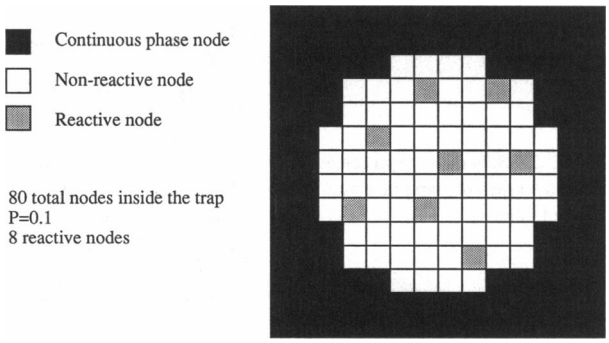

FIGURE 3 Computational representation of a trap with a diameter of 10 nodes (yielding 80 total nodes displayed as 80 white or gray boxes). The reaction probability is 0.1, so 10% of the nodes are reactive, represented by the 8 gray boxes. Black regions represent the inert continuous phase outside of the trap.

RESULTS AND DISCUSSION

The overall reaction rate constant has been evaluated for varying volume fraction of traps, trap reaction probabilities, particle diffusivities, and placement of traps. Results are presented as kr_t^2/D_e where k is the calculated rate constant and D_e is the particle effective diffusivity in the material, calculated from our previously reported scaling relationship (Riley et al., 1994). The normalized rate constant is analogous to a Thiele modulus, which measures the ratio of the rate of reaction to the rate of diffusion in heterogeneous catalysts (Froment and Bischoff, 1990). An alternative normalization

would be to use k/k_s; however, k_s (the Smoluchowski limit) is appropriate only for instantaneous reactions. The kr_t^2/D_e normalization is a more general approach that is valid regardless of P and hence is used here.

Nonoverlapping traps

Particle diffusion and reaction in NT structures are investigated for reaction probabilities (P) ranging from 0.001 to 1.0. The normalized rate constant increases with increasing trap fractions and reaction probability (Fig. 4 *a*) and increases more quickly with ϕ at high P than at low P. For $P = 1.0$, particle-trap reactions are instantaneous and the process is diffusion limited. At low P, particles spend a long time in the traps before reacting and the process is reaction limited. In this case, the rate constant becomes more dependent on individual trap reactivities than on the fraction of traps because particles may visit several traps before reacting.

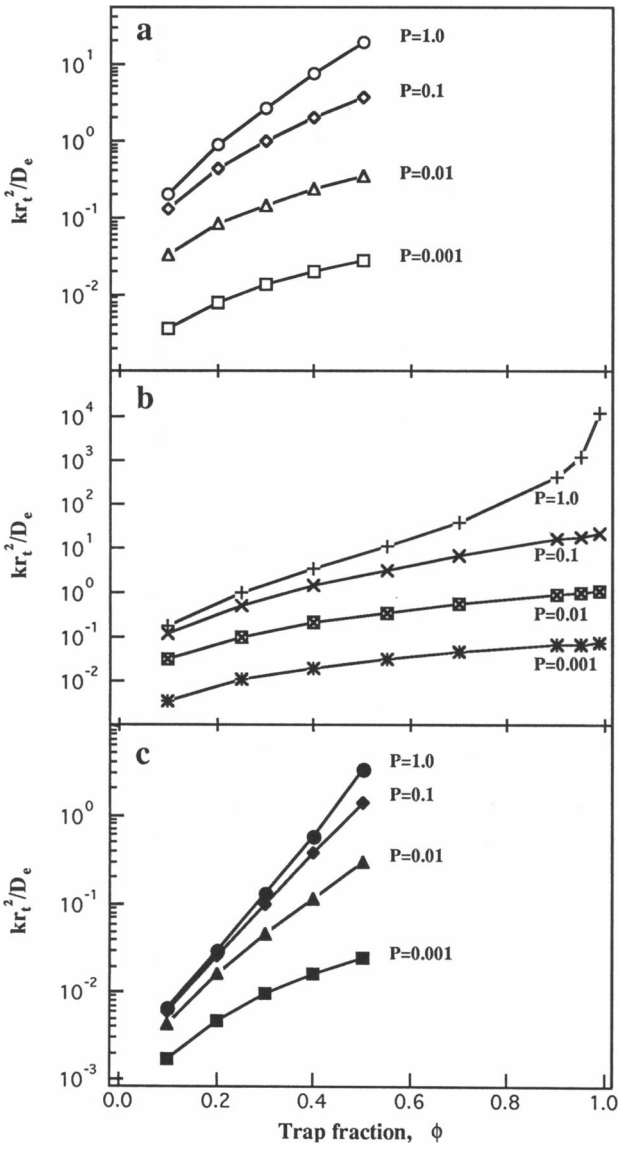

FIGURE 4 Normalized rate constants for several structures with four reaction probabilities: (*a*) NT with $P = 1.0$ (○); $P = 0.1$ (◇); $P = 0.01$ (△); $P = 0.001$ (□). (*b*) OT with $P = 1.0$ (+); $P = 0.1$ (x); $P = 0.01$ ⊠; $P = 0.001$ (✱). (*c*) CT with $P = 1$ (●); $P = 0.1$ (◆); $P = 0.01$ (▲); $P = 0.001$ (■).

Overlapping traps

Overlapping, randomly positioned traps are also investigated with $0.001 \leq P \leq 1.0$ and trap fractions up to 0.99 (Fig. 4 *b*). For high reaction probabilities ($P = 0.1$), the normalized rate constant increases with increasing trap fraction and reaction probability. For $P = 1.0$, as ϕ approaches 1, the rate constant becomes very large because nearly all of the sites are reactive. In such a case, particles initiate close to reactive sites. For $P \leq 0.1$, the normalized rate constant increases slowly with ϕ and approaches a finite maximum that depends on P; for example, with $P = 0.1$, kr_t^2/D_e gradually increases with ϕ toward a maximum of approximately 20. As with NT, high P corresponds to diffusion-limited conditions and low P corresponds to reaction-limited conditions.

Comparison with a single-conductive phase model

Our model can be contrasted with the model of Torquato and Avellaneda (1991) who investigated a system of traps in which particles that did not react bounced off of a trap instead of traveling into the trap. For the case of $P = 1.0$, with NT structures and with OT structures, the two models yield very similar rate constants because in both cases particles immediately react on the surface of traps. For $P = 0.1$, our model yields rate constants that are approximately an order of magnitude greater than those obtained by Torquato and Avellaneda. This difference can be anticipated by comparing what happens when particles on the surface of a trap do not react. In the Torquato and Avellaneda model, the particle would bounce off of a trap and must again diffuse to the surface of this trap or another trap before reacting. In our model, a particle is translated into a trap and so remains in the vicinity of reactive sites. This particle likely will react in a shorter time than the particle in the Torquato and Avellaneda model, hence our rate constants are somewhat larger.

Clustered traps

Structures with traps clustered in groups of 50 are evaluated for $P = 1.0$, 0.1, 0.01, and 0.001 and trap fractions from 0.10 to 0.50 (Fig. 4 *c*). The normalized rate constant increases sharply with ϕ for $P = 0.01$ but somewhat more slowly for $P = 0.001$. For trap fractions lower than 0.3, the normalized rate constant is nearly the same for $P = 1.0$ and $P = 0.1$. Clustering of traps segregates the reactive sites in a few regions of the structure, leaving large regions of trap-free area. When trap fractions are low, particles require significant time to diffuse through the nonreactive regions before reaching the surface of a trap. When a particle approaches a trap, it will also be in the vicinity of many other traps, so the particle most

likely will react in that region. Whether P is 1.0 or 0.1 has little effect on the time it takes the particle to react in comparison with the diffusional time required to reach the cluster. Under these conditions the process is diffusion limited. For trap fractions greater than approximately 0.3, the trap-free regions are small and particles spend a short time diffusing in trap-free areas. Accordingly, the reaction probability again controls the value of the rate constant. For low P, the rate constant is very dependent on P (as observed for NT and OT) and there is a significant difference between results with $P = 0.01$ and $P = 0.001$. In this case the process is reaction limited.

COMPARISON OF STRUCTURES

When directly comparing the three structures for the same trap fraction and reaction probability, the normalized rate constants are always highest in the NT system and lowest in the CT system (Fig. 5). Results for OT are somewhat lower than those for NT, in agreement with the trends reported by Richards (1987) and Miller and co-workers (1991) for diffusion-limited ($P = 1.0$) conditions. With $P = 1.0$ and a low trap fraction ($\phi = 0.1$), the NT and OT systems have similar normalized rate constants (Fig. 5 *a*), but as the trap fraction increases, normalized rate constants for NT increase more quickly than those for OT. Differences between NT and OT become smaller at lower P and for $P \leq 0.01$ their rate constants are nearly the same (Fig. 5, *b* and *c*) for all ϕ.

Normalized rate constants for CT with $P = 0.1$ are much lower than those for NT and OT (Fig. 5 *a* and *b*), suggesting that for high P the structure has a large effect on the rate constant. Richards (1987) reported that for $P = 1.0$, clustering of traps reduced the rate constant (as compared with rate constants obtained for unclustered traps). In our study, the difference between rate constants for CT and NT is as much as 1.5 orders of magnitude at $\phi = 0.1$ and $P = 1.0$. Smaller deviations are observed at higher ϕ and lower P. At high ϕ, the NT and CT structures are relatively similar because trap-free areas become smaller as the parking limit (approximately at $\phi = 0.55$ in two dimensions (Onoda and Liniger, 1986)) is approached. At high ϕ (>0.4), a structure is composed of many traps that are close together so that it is difficult to distinguish between clustered and unclustered traps. Particles most likely initiate close to traps, so it becomes immaterial whether the traps are clustered or not. For $P = 0.01$ and $\phi = 0.1$, normalized rate constants for CT are approximately an order of magnitude smaller than those for NT, but at $\phi = 0.5$ become nearly the same. When $P = 0.001$ (Fig. 5 *c*), the normalized rate constants for CT are similar to those for NT and OT. At low P, the process is reaction limited, the individual trap reactivity dominates the reaction behavior, and the structure has little effect on the rate constant.

The trends in predicted rate constants can be explained in terms of the segregation of reactive traps in the three different structures. The traps in NT and OT are evenly distributed,

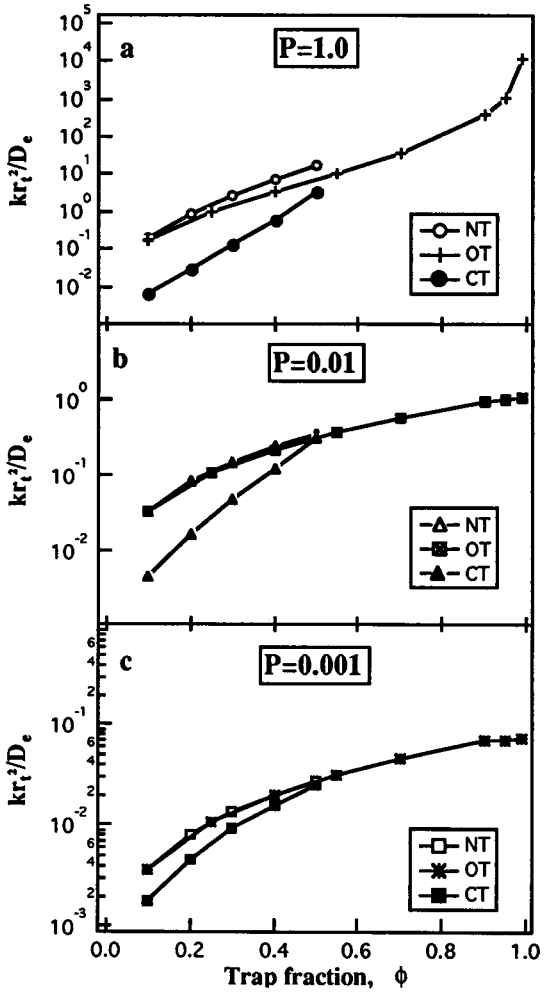

FIGURE 5 Comparison of the normalized rate constants for three structures, NT, OT, and CT. (*a*) $P = 1.0$, (*b*) $P = 0.01$, and (*c*) $P = 0.001$. At high reaction probabilities ($P \geq 0.1$), the structure is highly important in determining the normalized rate constant, but at lower reaction probabilities ($P < 0.1$), structural effects are less important. Note that the scales are different for each panel.

whereas the traps in CT are segregated into small groups. When $P = 1.0$, reactions are instantaneous and the overall process is diffusion limited. The controlling parameter is the trap surface area (S_a) accessible to diffusing particles. For NT this is:

$$S_a = 2\pi r_t N, \tag{7}$$

but for OT this is somewhat lower as a result of the overlap (Chiew and Glandt, 1983):

$$S_a = 2\pi r_t N \exp[-\pi N r_t^2/L^2]. \tag{8}$$

This difference in surface area is reflected in the trends observed in the rate constants of NT and OT. For CT the trap surface is the same as for NT, but the accessible surface is much smaller for CT because most particles react at the outer edges of a cluster. Many traps are buried at the center of a cluster and are not accessible to particles. These trends in the rate constants agree with the results of Zheng and Chiew

(1990) and Miller and Torquato (1989) who reported that the reaction rate for perfect traps ($P = 1.0$) increases with increasing surface area. With $P < 1.0$, the trap surface effect becomes less important because particles can diffuse into the traps before reacting. The reaction step is a greater limitation than the diffusive supply of particles to the trap surface and the fraction of reactive sites becomes more important than the placement of sites.

To better compare the results for the various structures, reaction probabilities, and trap fractions, results are presented in Fig. 6 in terms of absolute rate constants (not normalized) versus the fraction of total reactive sites, defined as the product of the trap fraction and the reaction probability, $P\phi$. Also included are the rate constants for systems in which single node reactive sites are randomly distributed throughout the computational domain occupying an area fraction equal to P. The rate constants for the random distribution of reactive sites serves as an upper bound on the rate constant for a given total fraction of reactive sites. OTs approach the limit at high ϕ because for both cases $P\phi \rightarrow 1$ so $k \rightarrow \infty$. For random reactive sites with $P < 0.05$, the rate constant k is proportional to P. The lowest rate constants for CT (obtained for $\phi = 0.1$) are quite similar at this scale and are far below the lowest values obtained for NT and OT even at $P = 0.001$. Note that the same value of the rate constant can be obtained for many different conditions. For example, $k = 0.002$ can be achieved with CT $\phi = 0.40$, $P = 1.0$; NT $\phi = 0.20$, $P = 0.1$; and many other combinations.

Effect of trap size

The results discussed so far indicate that trap clustering has a large effect on lowering the rate constant. The trap clustering algorithm generates clusters that are generally circular, and the CTs could be regarded as very large traps, each the size of a cluster (see Fig. 2). To further characterize the influence of structure on diffusion and reaction, the effect of trap size on the overall rate constant was investigated for uniformly distributed, nonoverlapping traps of different sizes. Results are presented in Fig. 7 as absolute rate constants for three trap sizes: small, $r_t = 3.75$ nodes; medium, $r_t = 7.5$ nodes (used previously); and large, $r_t = 15$ nodes. As expected for a given ϕ and P, the highest rate constants are obtained for small traps. To fill a given area fraction, structures consisting of small traps will require a larger number of traps than will a large trap structure, giving the small trap structure a greater surface area than the large trap structure. Small traps will tend to be more evenly distributed over the structure, and trap-free regions will be correspondingly small. Particles are likely initiated close to traps and so react quickly. At the same ϕ, a structure with large traps may have large trap-free regions, and particles may take a long time to react. The effects of trap size are greatest for $P = 1.0$ (Fig. 7 *a*) because reactions are fast and the surface area of traps is important. At lower reaction probabilities, $P \leq 0.01$ (Fig. 7 *b*), the effects of structure on reactivity decrease dramatically because particles diffuse farther and sample a larger portion of their environment. As a result, the rate constants for the three trap sizes become similar at these less reactive conditions.

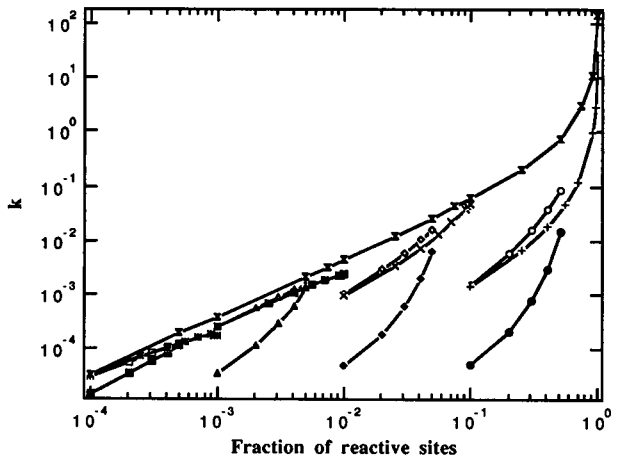

FIGURE 6 Absolute rate constants for the NT, OT, and CT structures along with rate constants for randomly placed reactive sites (I) as a function of the fraction of reactive sites $P\phi$. Symbols are as used for Fig. 4.

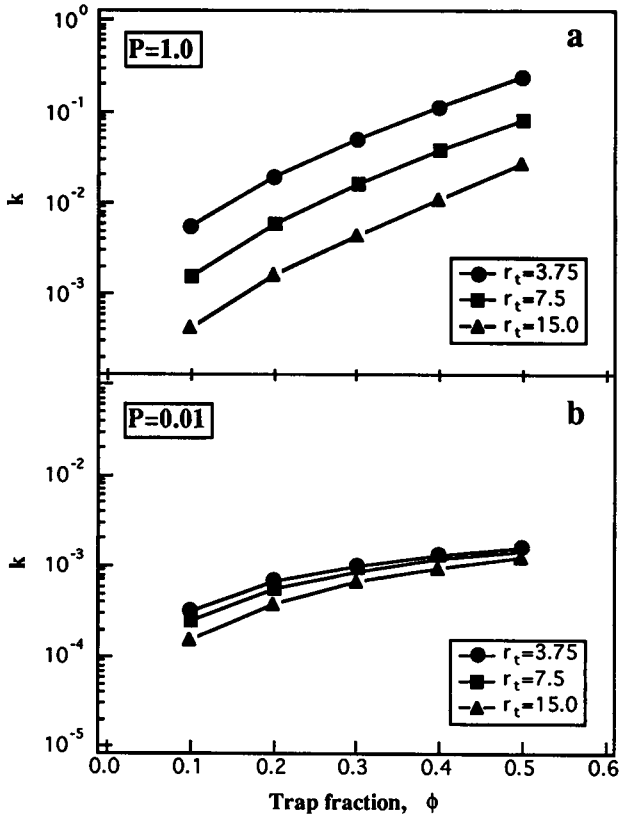

FIGURE 7 Effect of trap size on absolute rate constants for small ($r_t = 3.75$), medium ($r_t = 7.5$), and large ($r_t = 15$) traps in a NT structure. Medium-sized traps are the same as used in Figs. 4–6. Results are presented for (*a*) $P = 1.0$ and (*b*) $P = 0.01$.

Effect of D_0/D_c

When particles are allowed to enter the traps ($P < 1.0$), they diffuse in the traps with a diffusion coefficient, D_c, that is different than that in the continuous phase, D_0. Previous results in this paper correspond to materials with a diffusivity ratio of $D_0/D_c = 4$, a value that is representative of diffusion in animal cells immobilized in a gel matrix (Chresand et al., 1988). The effect of the diffusivity ratio on the rate constant has been evaluated with NT structures with different diffusivity ratios. Absolute rate constants for NT with $D_0/D_c = 1$, 4, and 10 are presented in Fig. 8. These ratios were achieved by changing D_c while keeping D_0 constant. The case of $P = 1.0$ is omitted because particles do not enter the traps and k is independent of D_0/D_c. For $D_0/D_c = 1$, there is no reduction in the particle diffusivity upon entering the trap, whereas $D_0/D_c = 10$ serves as a reasonable lower bound for biological materials that allow some measure of transport in all phases. A decrease in D_0/D_c from 10 to 1 increases the rate constant because particles diffuse more quickly in the traps, thus reducing the time required by a particle to encounter a reactive site. For lower values of P, D_0/D_c has a stronger effect on the rate constant because particles travel a long distance before reacting and spend more time within the traps.

Given the large number of parameters affecting the reactive behavior of the system discussed here, it is tempting to search for a simple relationship to predict rate constants for a wide range of conditions. An intuitive approach suggested by several authors (Cussler, 1984; Berg and von Hippel, 1985) is to assume that diffusion and reaction processes occur in series and can be expressed as:

$$1/k = 1/k_s + 1/k_r, \tag{9}$$

where k_s is the Smoluchowski limit and k_r is the intrinsic trap rate constant (Berg and von Hippel, 1985). Equation 9 implies that there exists a distinct diffusion time for the transport of particles to traps ($1/k_s$) and a separate time for the particle-trap reaction ($1/k_r$) and that the total time for the process is the sum of these individual steps. Unfortunately, such a simple phenomenological model does not capture the mechanisms in the system investigated here because, for low P, particles can walk in and out of traps without reacting, violating the seriality condition. Additionally, this model does not explicitly account for possible changes in D_0/D_c. To accurately model this behavior, one must have the diffusion time for particle transport to the surface of the trap in which the particle reacts and have the reaction time once inside the trap. These mechanisms are not easily captured by analytical relationships and therefore force us to resort to MC simulations.

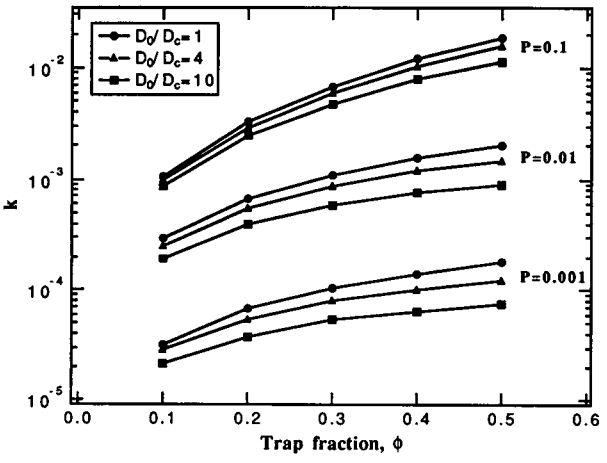

FIGURE 8 Effect of the diffusivity ratio (D_0/D_c) on the absolute rate constant for NT structures with three different reaction probabilities. The case of $P = 1.0$ is excluded because, for this case, k is independent of D_0/D_c.

CONCLUSIONS

A MC simulation has been developed to calculate rate constants for diffusion and reaction in two-dimensional biological systems. The results presented here can be used to answer several questions posed earlier. The system structure, as determined by the placement of traps, indeed influences the rate constants, but such effects are strong only when the traps are highly reactive. As the probability of reaction within a trap decreases, the effect of the material structure decreases. Structures with homogeneous distributions of reactive sites have the highest rate constants. At a given trap fraction, small traps will be more evenly distributed than large traps because of the relative number of traps, and so the former yields higher rate constants. The largest rate constants were obtained for randomly distributed reactive sites that are essentially very small traps. Among the structures with the same trap size, a system with nonoverlapping traps has the highest accessible surface area and therefore exhibits the largest rate constants. Clustering of traps decreases the accessible trap surface and leads to the lowest rate constants. Overlapping of traps yields a system with intermediate accessible surface area and hence intermediate rate constants. A large number of structural and reactive conditions may produce similar overall rate constants, so it is imperative to know not only the fraction of reactive traps but also their placement when extrapolating macroscopic rate constants to individual trap rate constants.

Information on the effect of structure on reactivity can be useful in analyzing biological systems. Our results show that clustered traps have much lower reactivity than unclustered traps, which can have practical consequences. DeFelice (1993) states that Ca channels cluster on the cell surface, creating an interaction of subunits that leads to cooperativity. Clustering could produce local regions of high channel density and regions of low channel density that, in light of our results, could also affect the rate at which Ca reaches the clusters of channels and ultimately traverses the cell membrane. Similar arguments can be applied to the transport and reaction of solutes in the cell interior, in multicell tumors, and in other similar systems.

This work was supported by a grant from the National Science Foundation (BCS 92–10540) to H.M.B. and by grants from the Exxon Education Foun-

dation and from the Merck Foundation to F.J.M. M.R.R. gratefully acknowledges Exxon Research and Engineering Company for supporting several summer internships.

REFERENCES

Axelrod, D., and M. D. Wang. 1994. Reduction-of-dimensionality kinetics at reaction-limited cell surface receptors. *Biophys. J.* 66:588–600.

Baldo, M., A. Grassi, and A. Raudino. 1991. Diffusion-controlled reactions among ligands and receptor clusters: effects of competition for ligands. *J. Phys. Chem.* 95:6734–6740.

Berg, O. G., and P. H. von Hippel. 1985. Diffusion-controlled macromolecular interactions. *Annu. Rev. Biophys. Chem.* 14:131–160.

Carlsson, J., and U. Brunk. 1977. The Fine Structure of three-dimensional colonies of human glioma cells in agarose culture. *Acta Pathol. Microbiol. Scand.* 85:183–192.

Carlsson, J., and J. M. Yuhas. 1984. Liquid-overlay culture of cellular spheroids. *Recent Res. Cancer Res.* 95:1–23.

Chiew, Y. C., and E. D. Glandt. 1983. The effect of structure on the conductivity of a dispersion. *J. Coll. Int. Sci.* 94:90–104.

Chresand, T. J., B. E. Dale, S. L. Hanson, and R. J. Gillies. 1988. A stirred bath technique for diffusivity measurements in cell matrices. *Biotech. Bioeng.* 32:1029–1036.

Coin, J. T., and J. S. Olson. 1979. The rate of oxygen uptake by human red blood cells. *J. Biol. Chem.* 254:1178–1190.

Cukier, R. I., and K. F. Freed. 1983. Diffusion controlled processes among stationary reactive sinks: effective medium aApproach. *J. Chem. Phys.* 78:2573–2578.

Cussler, E. L. 1984. Diffusion: Mass Transfer in Fluid Systems, 1st ed. Cambridge University Press, New York. 325–345.

DeBacker, L., and G. Baron. 1993. Effective diffusivity and tortuosity in a porous glass immobilization matrix. *Appl. Microb. Biotech.* 39:281–284.

de Beer, D., P. Stoodley, F. Roe, and Z. Lewandowski. 1994. Effects of biofilm structures on oxygen distribution and mass transport. *Biotech. Bioeng.* 43:1131–1138.

DeFelice, L. J. 1993. Molecular and biophysical view of the Ca channel: a hypothesis regarding oligomeric structure, channel clustering, and macroscopic current. *J. Membr. Biol.* 133:191–202.

Dwyer, J. D., and V. A. Bloomfield. 1993. Brownian dynamics simulations of probe and self-diffusion in concentrated protein and DNA solutions. *Biophys. J.* 65:1810–1816.

El-Kareh, A. W., S. L. Braunstein, and T. W. Secomb. 1993. Effect of cell arrangement and interstitial volume fraction on the diffusivity of monoclonal antibodies in tissue. *Biophys. J.* 64:1638–1646.

Fixman, M. 1984. Absorption by static traps: initial-value and steady-state problems. *J. Chem. Phys.* 81:3666–3677.

Fleischaker, R. J., Jr., and A. J. Sinskey. 1981. Oxygen demand and supply in cell culture. *Eur. J. Appl. Microbiol. Biotech.* 12:193–197.

Freyer, J. P., and R. M. Sutherland. 1986. Regulation of growth saturation and development of necrosis in EMT6/Ro multicellular spheroids by the glucose and oxygen supply. *Cancer Res.* 46:3504–3512.

Froment, G. F., and K. B. Bischoff. 1990. Chemical Reactor Design and Analysis, 2nd ed. John Wiley and Sons, New York.

Glacken, M. W., E. Adema, and A. J. Sinskey. 1988. Mathematical descriptions of hybridoma culture kinetics. I. Initial metabolic rates. *Biotech. Bioeng.* 32:491–506.

Grote, J., R. Susskind, and P. Vaupel. 1977. Oxygen diffusivity in tumor tissue (DS-carcinosarcoma) under temperature conditions within the range of 20–40°. *Pflugers Arch.* 372:37–42.

Hawboldt, K. A., N. Kalogerakis, and L. A. Behie. 1994. A cellular automaton model for microcarrier cultures. *Biotech. Bioeng.* 43:90–100.

Ho, C. S., and L.-K. Ju. 1988. Effects of microorganisms on effective oxygen diffusion coefficients and solubilities in fermentation media. *Biotech. Bioeng.* 32:313–325.

Jones, D. P. 1984. Effect of mitochondrial clustering on O_2 supply in hepatocytes. *Am. J. Physiol.* 247:C83-C89.

Joshi, G. C., R. Bhatnagar, S. Doraiswamy, and N. Periasamy. 1990. Diffusion-controlled reactions: transient effects in the fluorescence quenching of indole and *N*-acetyltryptophanamide in water. *J. Phys. Chem.* 94:2908–2914.

Kargacin, G. J. 1994. Calcium signaling in restricted diffusion spaces. *Biophys. J.* 67:262–272.

Karel, S. F., S. B. Libicki, and C. R. Robertson. 1985. The immobilization of whole cells: engineering principles. *Chem. Eng. Sci.* 40:1321–1354.

Kim, I. C., and S. Torquato. 1991. Effective conductivity of suspensions of hard spheres by brownian motion simulation. *J. Appl. Phys.* 69: 2280–2289.

Lee, S. B., and S. Torquato. 1988. Porosity for the penetrable-concentric-shell model of two-phase disordered media: computer simulation results. *J. Chem. Phys.* 89:3258–3263.

Lee, S. B., I. C. Kim, C. A. Miller, and S. Torquato. 1989. Random-walk simulation of diffusion-controlled processes among static traps. *Phys. Rev. B.* 39:11833–11839.

Libicki, S. B., P. M. Salmon, and C. R. Robertson. 1988. The effective diffusive permeability of a nonreacting solute in microbial cell aggregates. *Biotech. Bioeng.* 32:68–85.

Mahama, P. A., and J. J. Linderman. 1994. A Monte Carlo study of the dynamics of G-protein activation. *Biophys. J.* 67:1345–1357.

McGee, M. P., L. C. Li, and H. Xiong. 1992. Diffusion control in blood coagulation. *J. Biol. Chem.* 267:24333–24339.

Miller, C. A., and S. Torquato. 1989. Diffusion-controlled reactions among spherical traps: effect of polydispersity in trap size. *Phys. Rev. B.* 40: 7101–7108.

Miller, C. A., I. C. Kim, and S. Torquato. 1991. Trapping and flow among random arrays of oriented spheroidal inclusions. *J. Chem. Phys.* 94: 5592–5598.

Muthukumar, M. 1982. Concentration dependence of diffusion controlled processes among static traps. *J. Chem. Phys.* 76:2667–2671.

Northrup, S. H., and H. P. Erickson. 1992. Kinetics of protein-protein association explained by Brownian dynamics computer simulation. *Proc. Natl. Acad. Sci. USA.* 89:3338–3342.

Onoda, G. Y., and E. G. Liniger. 1986. Experimental determination of the random-parking limit in two dimensions. *Phys. Rev. A.* 33:715–716.

Ozturk, S. S., and B. O. Palsson. 1991. Growth, metabolic, and antibody production kinetics of hybridoma cell culture. I. Analysis of data from controlled batch reactors. *Biotech. Prog.* 7:471–480.

Reyes, S. C., and E. Iglesia. 1991. Effective diffusivities in catalyst pellets: new model porous structures and transport simulation techniques. *J. Catal.* 129:457–472.

Reyes, S., and K. F. Jensen. 1985. Estimation of effective transport coefficients in porous solids based on percolation concepts. *Chem. Eng. Sci.* 40:1723–1734.

Richards, P. M. 1986a. Diffusion to finite-size traps. *Phys. Rev. Lett.* 56: 1838–1841.

Richards, P. M. 1986b. Diffusion and trapping at arbitrary trap size and concentration. *J. Chem. Phys.* 85:3520–3529.

Richards, P. M. 1987. Diffusion to nonoverlapping or spatially correlated traps. *Phys. Rev. B.* 35:248–256.

Riley, M. R., F. J. Muzzio, H. M. Buettner, and S. C. Reyes. 1994. Monte Carlo calculation of effective diffusivities in two-and three-dimensional heterogeneous materials of variable structure. *Phys. Rev. E.* 49: 3500–3503.

Riley, M. R., F. J. Muzzio, H. M Buettner, and S. C. Reyes. 1995. Diffusion in heterogenous media: application to immobilized cell systems. *AIChE J.* 41:691–711.

Rubinstein, J., and S. Torquato. 1988. Diffusion-controlled reactions: mathematical formulation, variational principles, and rigorous bounds. *J. Chem. Phys.* 88:6372–6380.

Saxton, M. J. 1989. Lateral diffusion in an archipelago: distance dependence of the diffusion coefficient. *Biophys. J.* 56:615–622.

Saxton, M. J. 1992. Lateral diffusion and aggregation: a Monte Carlo study. *Biophys. J.* 61:119–128.

Saxton, M. J. 1993a. Lateral diffusion in an archipelago: single-particle diffusion. *Biophys. J.* 64:1766–1780.

Saxton, M. J. 1993b. Lateral diffusion in an archipelago: dependence on tracer size. *Biophys. J.* 64:1053–1062.

Saxton, M. J. 1994. Anomalous diffusion due to obstacles: a Monte Carlo study. *Biophys. J.* 66:394–401.

Scott, C. D., C. A. Woodward, and J. E. Thompson. 1989. Solute diffusion in biocatalyst gel beads containing biocatalysis and other additives.

Enzyme Microb. Technol. 11:258–263.

Sutherland, R. M., and R. E. Durand. 1984. Growth and cellular characteristics of multicell spheroids. *Recent Res. Cancer Res.* 95:24–49.

Szabo, A. 1989. Theory of diffusion-induced fluorescence quenching. *J. Phys. Chem.* 93:6929–6939.

Tabor, D. 1969. Gases, Liquids, and Solids, 2nd ed. Cambridge Press, Cambridge. 84–86.

Torquato, S., and M. Avellaneda. 1991. Diffusion and reaction in heterogeneous media: pore size distribution, relaxation times, and mean survival time. *J. Chem. Phys.* 95:6477–6489.

Vaupel, P. 1976. Effect of percentual water content in tissues and liquids on the diffusion coefficients of O_2, CO_2, N_2, and H_2. *Pflugers Arch.* 361: 201–204.

Wohlpart, D., D. Kirwan, and J. Gainer. 1990. Effects of cell density and glucose and glutamine levels on the respiration rates of hybridoma cells. *Biotech. Bioeng.* 36:630–635.

Westrin, B. A., and A. Axelsson. 1991. Diffusion in gels containing immobilized cells: a critical review. *Biotech. Bioeng.* 38:439–446.

Zhao, S., and W. M. Reichert. 1994. Analysis of protein binding to receptor-doped lipid monolayers by Monte Carlo simulation. *Biophys. J.* 66: 305–309.

Zheng, L. H., and Y. C. Chiew. 1989. Computer simulation of diffusion-controlled reactions in dispersions of spherical sinks. *J. Chem. Phys.* 90:322–327.

Zheng, L. H., and Y. C. Chiew. 1990. Computer simulation of steady-state diffusion-controlled reaction rates in dispersions of static sinks: effect of sink size. *J. Chem. Phys.* 93:2658–2663.

Zygourakis, K., R. Bizios, and P. Markenscoff. 1991a. Proliferation of anchorage-dependent contact-inhibited cells. I. Development of theoretical models based on cellular automata. *Biotech. Bioeng.* 38:459–470.

Zygourakis, K., P. Markenscoff, and R. Bizios. 1991b. Proliferation of anchorage-dependent contact-inhibited cells. II. Experimental results and validation of the theoretical models. *Biotech. Bioeng.* 38:471–479.